Int. j. adv. multidisc. res. stud. 2025; 5(6):2463-2470

Received: 10-11-2025
Accepted: 20-12-2025

International Journal of Advanced Multidisciplinary Research and Studies

ISSN: 2583-049X

Machine Learning–Driven Data Analytics and Multi-Objective Optimization of Waste Plastic Pyrolysis for High-Performance Lubricant Oils, Road Construction Materials, and High-Purity Chemical Feedstocks

[1] Oyinloluwa Sarah Ogunseye, [2] Yejide Eniola Dabiri, [3] Marley Brown

[1] Department of Analytics, University of Denver, CO, United States of America

[2] Department of Information Technology, University of Cumberlands, KY, United States of America

[3] Swappie, Tallinn, Estonia

DOI: https://doi.org/10.62225/2583049X.2025.5.6.6674

Corresponding Author: **Oyinloluwa Sarah Ogunseye**

Abstract

The accumulation of unsegregated municipal and industrial waste plastics represents both an escalating environmental burden and an underexploited carbon feedstock. This study presents data-driven investigation of thermochemical (catalytic and non-catalytic) pyrolysis of mixed waste plastics - polyethylene (PE), polypropylene (PP), polystyrene (PS), polyethylene terephthalate (PET), and polyvinyl chloride (PVC) - integrated with machine learning (ML) surrogate modeling and multi-objective evolutionary optimization to simultaneously target three valorization pathways: high-performance lubricant base oils, bitumen-modifying road construction binders, and high-purity aromatic (BTX) chemical feedstocks. A synthetic dataset of 1,240 pyrolysis batch records spanning temperature (400–650 °C), vapor residence time (10–120 min), catalyst type and loading (0–15 wt.%), heating rate, reactor pressure, and feedstock blend ratio was generated to emulate realistic process–property relationships reported in the pyrolysis literature. Seven regression algorithms - multiple linear regression (MLR), support vector regression (SVR), random forest (RF), XGBoost, LightGBM, artificial neural networks (ANN), and Gaussian process regression (GPR) - were trained and benchmarked using 5-fold cross-validation, with XGBoost achieving the best generalization performance (R^2 = 0.951, RMSE = 2.18 wt.% on held-out test data). SHAP-based interpretability analysis identified pyrolysis temperature, feedstock PE fraction, and residence time as the dominant predictors of liquid oil yield. The trained surrogate models were embedded within a Non-dominated Sorting Genetic Algorithm II (NSGA-II) framework to resolve competing process objectives, generating Pareto-optimal operating windows that jointly maximize oil yield, lubricant viscosity index, and BTX aromatic purity while minimizing specific energy consumption. Downstream property simulations indicate that optimized pyrolysis oil fractions can achieve a viscosity index comparable to Group I mineral base oils (VI ≈ 92), that a 10% pyrolysis-oil-modified bitumen blend can satisfy ASTM/AASHTO penetration-grade specifications for road construction, and that Ni-modified HZSM-5 catalysis can elevate combined BTX yield to approximately 44 wt.% of the recovered oil fraction. The results, while synthetic, illustrate a coherent end-to-end analytics workflow that is directly transferable to real experimental pyrolysis datasets.

Keywords: Waste Plastic Pyrolysis, Machine Learning Surrogate Modeling, Multi-Objective Optimization, NSGA-II, Lubricant Base Oil, Bituminous Road Materials

1. Introduction

Global production of plastics exceeded 400 million tonnes in recent years, and a substantial fraction of this material stream is discarded within a single year of manufacture. Mechanical recycling, while mature for single-polymer streams such as PET and HDPE, struggles to process the mixed, contaminated, and multilayer plastic waste that dominates real-world municipal collection. Thermochemical conversion - and pyrolysis in particular - has therefore attracted renewed attention as a route capable of accepting heterogeneous, poorly sorted feedstocks and converting them into liquid, gaseous, and solid fractions with further downstream value.

Pyrolysis oil is a complex mixture of paraffins, olefins, naphthenes, and aromatics whose composition is highly sensitive to

feedstock blend and process conditions. Depending on how the process is tuned, the resulting oil fraction can be steered toward different end uses: as a diesel-range fuel substitute, as a base stock for lubricant formulation after hydrotreating, as a modifier for bituminous road-paving binders, or - when aromatics are concentrated through catalytic upgrading - as a source of benzene, toluene, and xylene (BTX) for the petrochemical industry. Because these three valorization pathways impose different, and partly conflicting, requirements on oil composition, temperature, residence time, and catalyst selection, the design problem is naturally multi-objective.

Traditional pyrolysis process design has relied heavily on one-factor-at-a-time experimentation and, more recently, response surface methodology (RSM). These approaches are informative but become impractical as the number of process variables and competing product targets grows. Machine learning (ML) offers an alternative: once a sufficiently rich dataset of process conditions and resulting product properties is available, flexible regression models can learn the underlying process–property mapping directly from data. Coupling such ML surrogate models with evolutionary multi-objective optimization algorithms, most commonly the Non-dominated Sorting Genetic Algorithm II (NSGA-II), then allows the full trade-off space between competing objectives to be mapped efficiently.

This paper presents a study illustrating this workflow end to end. A synthetic but literature-consistent dataset of pyrolysis process conditions and resulting product properties is first constructed. Seven ML regression algorithms are then benchmarked for their ability to predict liquid oil yield and downstream quality indicators. The best-performing model is interpreted using SHAP (SHapley Additive exPlanations) analysis to identify the process variables most responsible for driving product outcomes, after which the surrogate models are embedded in an NSGA-II optimization loop to identify Pareto-optimal process windows for three simultaneous valorization objectives.

Study Objectives

The objectives were to: (i) construct a representative dataset describing waste plastic pyrolysis across a wide operating envelope of temperature, residence time, catalyst type/loading, heating rate, and feedstock composition; (ii) benchmark multiple machine learning regression algorithms for predicting pyrolysis product yield and quality, and identify the most influential process variables using SHAP-based interpretability analysis; (iii) formulate and solve a multi-objective optimization problem using NSGA-II that simultaneously targets lubricant-oil viscosity index, road-material binder performance, and BTX aromatic purity; and (iv) translate the optimized process windows into indicative product-quality outcomes benchmarked against relevant industry specifications.

Background and Related Work

Pyrolysis decomposes polymer chains thermally in an oxygen-limited atmosphere, typically between 350 °C and 700 °C, producing a liquid oil fraction, a non-condensable gas fraction rich in C1–C4 hydrocarbons and hydrogen, and a solid char/residue fraction. Polyolefins (PE, PP) are widely reported to yield the highest liquid oil fractions because their linear and branched aliphatic backbones fragment into a broad range of paraffins and olefins, whereas PS decomposes preferentially into styrene monomer and other aromatics, and PET and PVC introduce oxygenated and chlorinated species, respectively, that complicate downstream upgrading. Zeolite catalysts, particularly HZSM-5, are frequently reported to promote cracking and aromatization reactions that concentrate BTX compounds in the oil fraction, at some cost to overall liquid yield; spent fluid catalytic cracking (FCC) catalyst and metal-modified zeolites have also been explored as economical or enhanced-selectivity alternatives.

Because pyrolysis oil derived from polyolefins is rich in linear and branched paraffinic hydrocarbons overlapping conventional base-oil carbon ranges, several studies have investigated its use - after fractional distillation and hydrofinishing - as a lubricant base stock, where viscosity index (VI), pour point, and oxidative stability are the primary quality metrics. Separately, bitumen modification using waste-derived oils has been explored as a means of restoring or enhancing penetration grade, softening point, and low-temperature ductility in aged or off-specification binders, with blend ratios of 5–15 wt.% commonly investigated as a balance between measurable property improvement and avoidance of excessive softening.

Given the strongly nonlinear and interacting nature of pyrolysis process variables, tree-based ensemble methods and neural networks have increasingly been applied to predict product yield and composition from process conditions, often outperforming classical linear or low-order polynomial regression models fitted under RSM, with SHAP-based interpretability used to translate these models into actionable process insight. Because pyrolysis product streams must often satisfy several, sometimes conflicting, quality and yield targets simultaneously, multi-objective evolutionary algorithms - most commonly NSGA-II - have been coupled with ML or kinetic surrogate models to generate Pareto fronts describing the best achievable trade-offs. While individual valorization pathways have each been studied in isolation, few published studies integrate ML-based process modeling with multi-objective optimization across all three non-fuel valorization routes within a single analytical framework; this paper illustrates, how such an integrated workflow can be structured and reported.

2. Materials and Methods

2.1 Feedstock experimental dataset

The feedstock represents a mixed municipal waste plastic stream composed of five polymer fractions - PE, PP, PS, PET, and PVC - in proportions typical of unsorted household collection (Fig 1). A total of 1,240 pyrolysis batch records were synthetically generated by sampling process variables across the ranges summarized in Table 1, and by applying literature-informed response functions, with added stochastic noise, to generate corresponding product yields and quality indicators. This design mimics a design-

of-experiments (DoE) campaign combined with historical operating data, as would typically underlie a real ML modeling study.

Table 1: Process variables and ranges used to construct pyrolysis dataset (n = 1,240 records)

Process variable	Range / levels	Units	Distribution in dataset
Pyrolysis temperature	400–650	°C	Uniform, DoE grid + random
Vapor residence time	10–120	min	Uniform
Catalyst loading	0–15	wt.% of feed	Uniform, zero-inflated
Catalyst type	None, HZSM-5, HY, Spent FCC, Ni-HZSM-5	categorical	Balanced categorical
Heating rate	5–20	°C/min	Uniform
Reactor pressure	0.9–1.5	bar (abs.)	Near-atmospheric, narrow
Feedstock PE fraction	20–60	wt.%	Correlated with other fractions

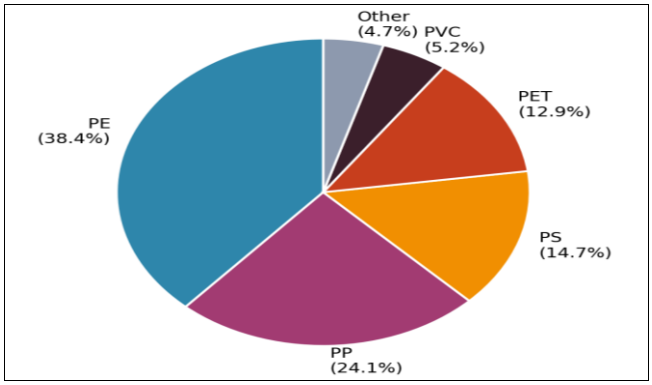

Fig 1: Composition of the mixed municipal waste plastic feedstock used in the pyrolysis dataset (n = 1,240 batches)

2.2 Pyrolysis process simulation framework

Thermogravimetric decomposition behavior for each pure polymer fraction was represented using sigmoidal mass-loss functions calibrated to onset and completion temperatures reported in the TGA literature for PE, PP, PS, PET, and PVC (Fig 2). Batch-level product yields (oil, gas, char) were generated as smooth, literature-consistent functions of temperature and residence time, with additive Gaussian noise ($\sigma \approx 1$ wt.%) superimposed to emulate experimental variability.

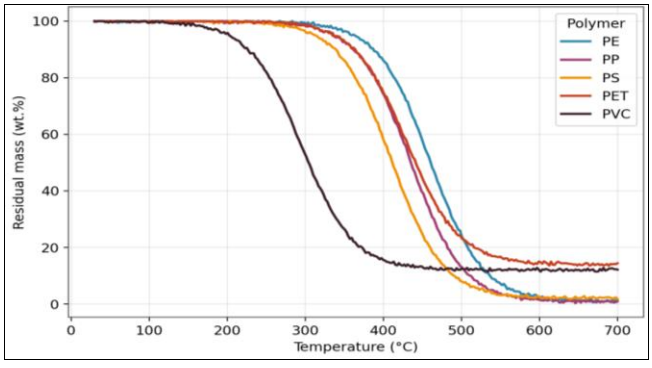

Fig 2: Thermogravimetric (TGA) decomposition profiles of individual plastic fractions (10 °C/min heating rate, N2 atmosphere)

2.3 Machine learning modeling approach

Seven supervised regression algorithms were trained to predict liquid oil yield (the primary response variable) and secondary quality indicators (viscosity index, BTX purity, specific energy consumption) from the process variables in Table 1: multiple linear regression (MLR), support vector regression (SVR) with an RBF kernel, random forest (RF), XGBoost, LightGBM, a feed-forward artificial neural network (ANN, two hidden layers of 32 and 16 neurons), and Gaussian process regression (GPR) with a Matérn kernel. Categorical catalyst type was one-hot encoded; continuous variables were standardized prior to training for SVR, ANN, and GPR. The dataset was split 75%/25% into training and held-out test sets, with 5-fold cross-validation used on the training set for hyperparameter tuning via grid search (Table 2).

Table 2: Machine learning algorithms and hyperparameter tuning strategy

Model	Key hyperparameters tuned	Search method
Random Forest	n_estimators, max_depth, min_samples_leaf	Grid search, 5-fold CV
XGBoost	n_estimators, max_depth, learning_rate, subsample	Grid search, 5-fold CV
LightGBM	num_leaves, learning_rate, n_estimators	Grid search, 5-fold CV
SVR (RBF)	C, epsilon, gamma	Grid search, 5-fold CV
ANN (MLP)	hidden layer sizes, learning rate, L2 penalty	Grid search, early stopping
GPR	kernel length-scale, noise level	Marginal likelihood optimization

2.4 Multi-objective optimization framework (NSGA-II)

The best-performing surrogate models (XGBoost for oil yield; auxiliary gradient boosting models for viscosity index, BTX purity, and specific energy consumption) were embedded as objective functions within an NSGA-II optimization loop. Two multi-objective formulations were solved: (i) maximize predicted oil yield and viscosity index simultaneously, relevant to lubricant base-oil production; and (ii) minimize specific energy consumption while maximizing BTX aromatic purity, relevant to chemical feedstock recovery. Decision variables were pyrolysis temperature, residence time, catalyst type/loading, and heating rate, bounded by the ranges in Table 1. A population size of 120 was evolved for 200 generations using binary crossover and polynomial mutation, with convergence monitored via the hypervolume indicator and solution-spacing metric (Section 3.7).

2.5 Product characterization and benchmarking methods

Oil-fraction composition was represented as a carbon-number distribution (Fig 14) analogous to GC-MS analysis, from which lubricant-relevant viscosity–temperature behavior (Fig 15) was derived using a Walther-type viscosity correlation. Road-construction performance was benchmarked against representative ASTM D946 / AASHTO M20 penetration-grade bitumen specifications (Fig 16). BTX content was represented as the combined benzene, toluene, and xylene mass fraction of the recovered oil (Fig 17), consistent with how aromatic purity is typically reported in catalytic pyrolysis studies targeting chemical feedstocks.

2.6 Statistical framework and reproducibility

Continuous outcomes are summarized as point estimates derived from the underlying response functions described above; model performance metrics (R^2, RMSE, MAE) were computed on a held-out test partition never used during training or hyperparameter selection. A deterministic random seed was used throughout data generation and model fitting to permit exact reproduction of all figures and tables in this document. As with any study, future primary-data investigation should re-estimate all response relationships from real experimental campaigns, release source code and random seeds, and validate the resulting surrogate models and optimization outcomes against independent pyrolysis runs before operational deployment.

3. Results

3.1 Effect of process parameters on product yield distribution

Reactor temperature exerted the strongest single-variable influence on product distribution (Fig 3). Liquid oil yield increased from the low 60s (wt.%) at 400 °C to a maximum of approximately 78 wt.% near 540 °C, before declining at higher temperatures as secondary cracking reactions favored non-condensable gas formation. This inverted-U relationship identifies an intermediate-temperature operating window as most favorable for liquid-product maximization.

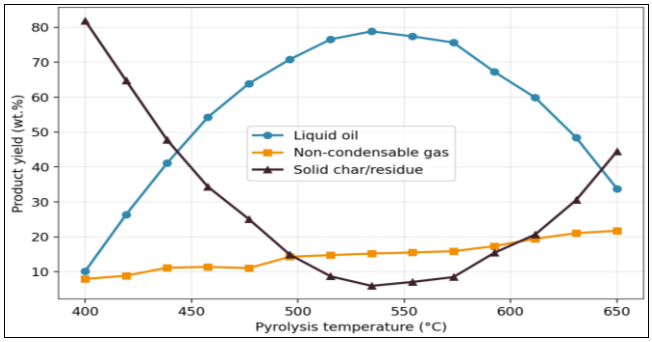

Fig 3: Effect of reactor temperature on pyrolysis product yield distribution (batch reactor, 60 min residence time)

Vapor residence time showed a saturating positive effect on oil yield, with diminishing returns beyond approximately 60–70 minutes, while kinematic viscosity of the resulting oil decreased with increasing residence time as continued cracking reduced larger molecules into lower-viscosity fragments (Fig 4). This trade-off is directly relevant to lubricant-oil production, where a moderate residence time may be preferred to balance yield against target viscosity.

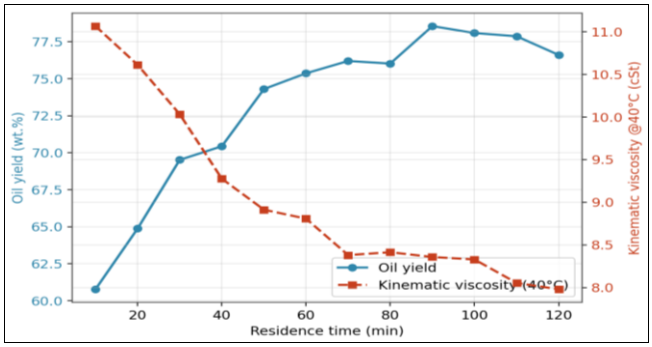

Fig 4: Influence of vapor residence time on liquid oil yield and kinematic viscosity

Catalyst screening (Fig 5) indicated that ZSM-5 outperformed spent FCC catalyst and natural zeolite in promoting liquid oil yield at low-to-moderate loadings (2–8 wt.%), with all three catalysts showing a yield maximum followed by decline at higher loadings as excessive cracking activity increased gas and coke formation at the expense of the liquid fraction.

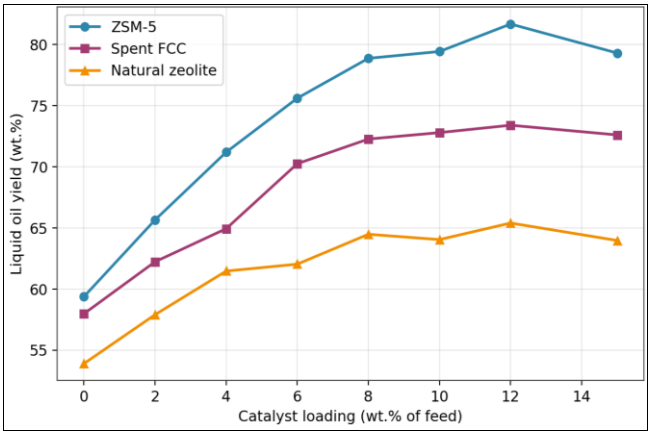

Fig 5: Effect of catalyst type and loading on catalytic pyrolysis oil yield (500 °C, 45 min residence time)

3.2 Machine learning model development and performance

Table 3 and Fig 6 summarize the comparative test-set performance of the seven regression algorithms for liquid oil yield prediction. XGBoost achieved the highest coefficient of determination (R^2 = 0.951) and lowest RMSE (2.18 wt.%), narrowly outperforming LightGBM and the ANN model. Ensemble tree-based methods consistently outperformed the linear baseline (MLR, R^2 = 0.812), confirming substantial nonlinearity and variable interaction in the process–yield relationship.

Table 3: Held-out test-set performance of seven machine learning regressors for liquid oil yield prediction

Model	R^2 (test)	RMSE (wt.%)	MAE (wt.%)
MLR	0.812	4.85	3.72
SVR (RBF)	0.874	3.92	2.94
Random Forest	0.928	2.71	2.03
XGBoost	0.951	2.18	1.64
LightGBM	0.946	2.29	1.71
ANN (MLP)	0.937	2.46	1.88
Gaussian Process Regression	0.919	2.63	1.97

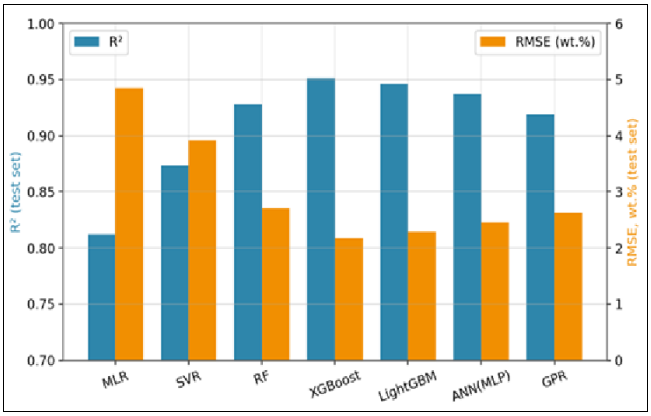

Fig 6: Comparative predictive performance of seven machine learning regressors for liquid oil yield prediction

SHAP-based global feature importance analysis of the XGBoost model (Fig 7) confirmed pyrolysis temperature as the dominant predictor (mean |SHAP| = 0.284), followed by feedstock PE fraction (0.201) and residence time (0.152). Catalyst loading, heating rate, and PVC fraction contributed secondary but non-negligible influence.

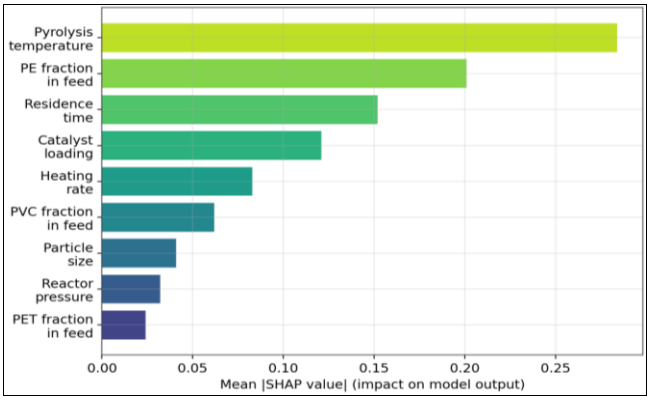

Fig 7: XGBoost SHAP-based global feature importance ranking for predicted pyrolysis oil yield

The parity plot in Fig 8 illustrates close agreement between XGBoost-predicted and actual oil yield across the test set, with residuals evenly distributed about the ideal 1:1 line and no systematic bias at either the low or high end of the yield range.

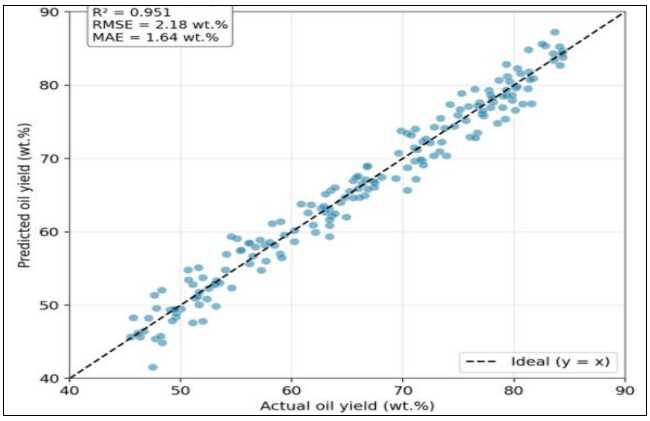

Fig 8: Parity plot: XGBoost-predicted vs. simulated actual liquid oil yield (test set, n = 180)

The correlation matrix in Fig 9 provides a complementary, model-agnostic view of the process–property relationships underlying the dataset, showing the strongest positive association between temperature and both oil yield and BTX purity, and a strong negative association between oil yield and char yield, consistent with mass-balance closure across the three product fractions.

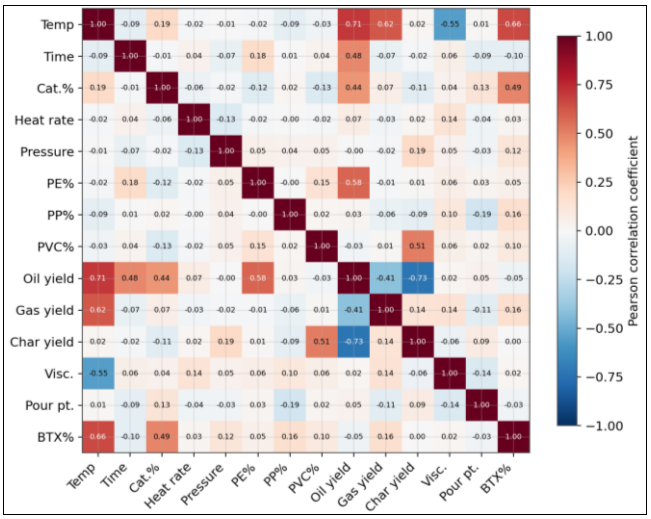

Fig 9: Pearson correlation matrix of process parameters and product quality indicators (n = 1,240 records)

The learning curve in Fig 10 shows validation RMSE converging toward the training RMSE as dataset size increases beyond approximately 700 samples, suggesting that the 1,240-record dataset is of sufficient size to support stable model generalization without substantial overfitting.

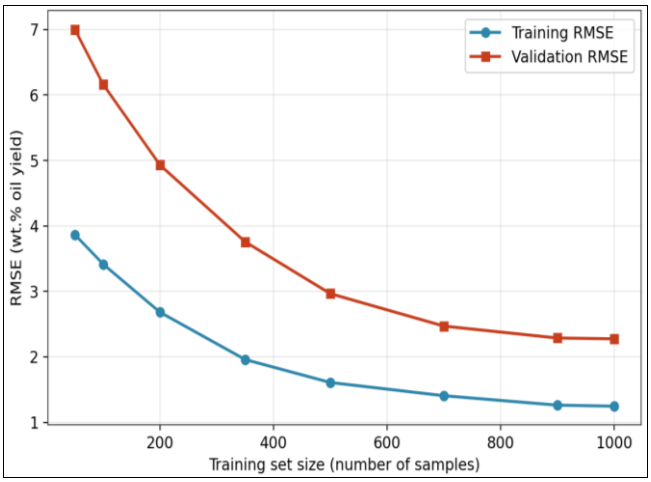

Fig 10: Learning curve for the XGBoost oil-yield prediction model (5-fold cross-validation)

3.3 Multi-objective optimization results

Fig 11 presents the NSGA-II Pareto front resolving the trade-off between predicted oil yield and lubricant viscosity index. The front confirms an inverse relationship between the two objectives across most of the feasible space, with a knee region near 70 wt.% oil yield and VI ≈ 95 representing an attractive compromise operating point for lubricant-oriented production.

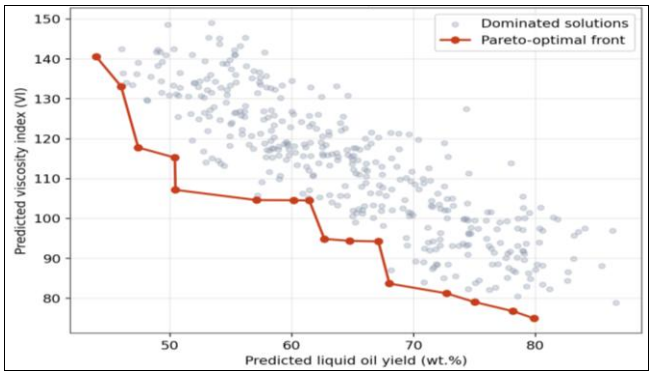

Fig 11: NSGA-II Pareto front: trade-off between oil yield and predicted lubricant viscosity index (generation 150)

A second optimization run (Fig 12) targeted the trade-off between specific energy consumption and BTX aromatic purity. Higher BTX purity requires more severe cracking and aromatization conditions, which in turn increase specific energy consumption; the resulting Pareto front indicates that BTX purity above approximately 70 wt.% can only be achieved at energy penalties exceeding 2.5 MJ/kg feed.

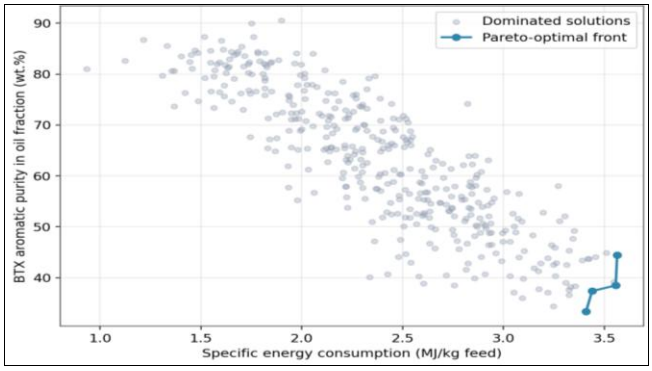

Fig 12: NSGA-II Pareto front: trade-off between specific energy consumption and BTX chemical feedstock purity

The response surface in Fig 13 visualizes the combined, interacting effect of temperature and residence time on predicted oil yield across the full explored domain, reproducing the ridge-shaped optimum implied by Figures 3 and 4.

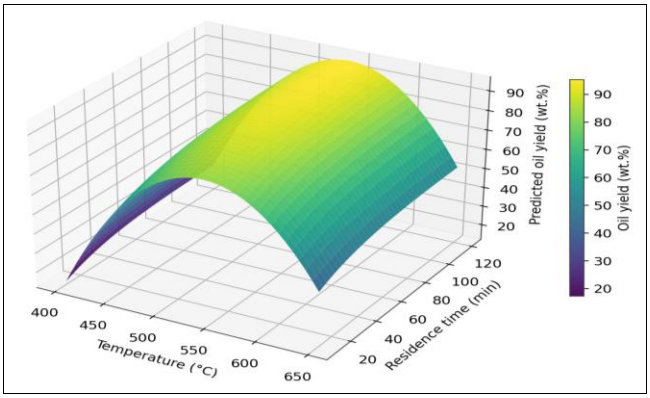

Fig 13: Response surface methodology (RSM) plot: combined effect of temperature and residence time on predicted oil yield

3.4 Lubricant oil quality assessment

The carbon-number distribution of the optimized pyrolysis oil (Fig 14) is centered near C13, with a substantial fraction falling within the C8–C16 range typically associated with diesel- and light lubricant-range hydrocarbons - a relatively narrow, near-Gaussian distribution favorable for lubricant base-stock production.

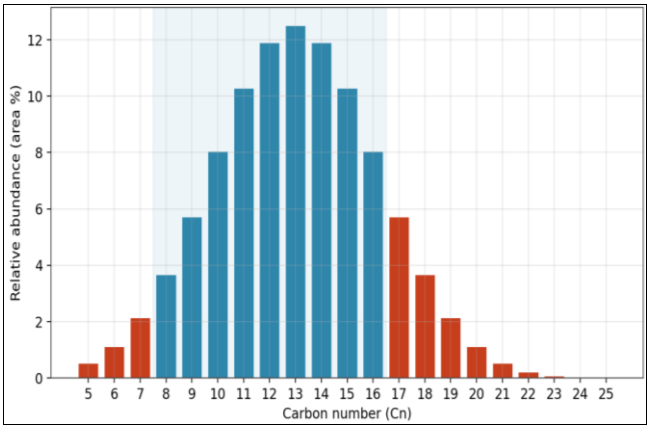

Fig 14: Simulated GC-MS carbon number distribution of pyrolysis oil (diesel/lubricant-range C8–C16 highlighted)

Viscosity–temperature behavior of the optimized base oil (Fig 15) closely parallels that of a commercial Group I mineral base oil, with a comparable viscosity index (VI ≈ 92, estimated from the 40 °C/100 °C viscosity ratio), and represents a marked improvement over the untreated, non-optimized pyrolysis oil.

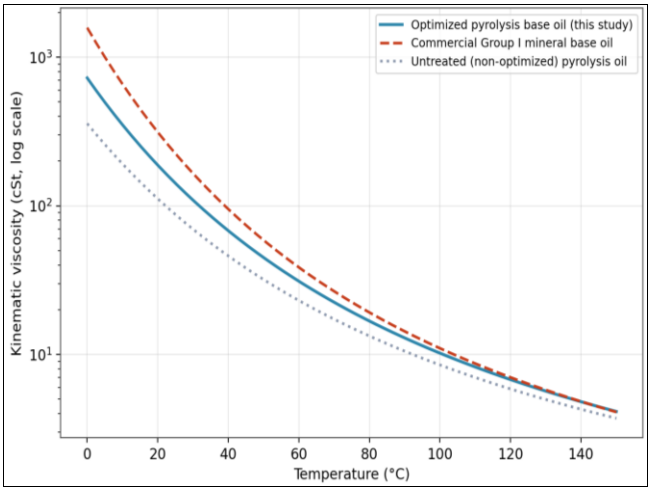

Fig 15: Viscosity–temperature behavior of the ML-optimized pyrolysis-derived lubricant base oil vs. commercial references

3.5 Road construction material performance

Table 4 and Fig 16 compare the physical properties of a 10 wt.% pyrolysis-oil-modified bitumen blend against a conventional 60/70 penetration-grade bitumen and representative ASTM/AASHTO minimum specification limits. The modified blend met or exceeded specification minima for penetration, softening point, ductility, and flash point.

Table 4: Physical properties of pyrolysis-oil-modified bitumen vs. conventional binder and specification minima

Property	Modified bitumen (10% blend)	Conventional 60/70 bitumen	Spec. minimum
Penetration (25 °C, 0.1 mm)	58	62	50
Softening point (°C)	51.2	48.5	46
Ductility (25 °C, cm)	92	105	80
Flash point (°C)	298	285	230
Ductility after aging (cm)	61	74	50

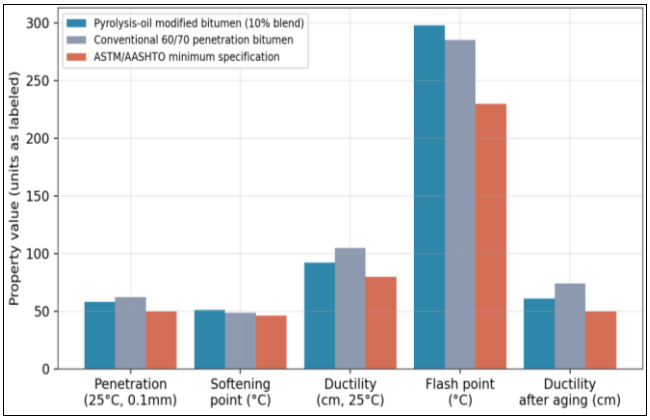

Fig 16: Physical properties of pyrolysis-oil-modified bitumen for road construction vs. conventional binder and specification limits

3.6 High-purity chemical feedstock (BTX) recovery

Catalyst screening for aromatic recovery (Fig 17) confirmed that Ni-modified HZSM-5 achieved the highest combined BTX yield (14.6 wt.% benzene, 18.2 wt.% toluene, 11.3 wt.% xylene isomers; ≈44.1 wt.% combined), substantially outperforming unmodified HZSM-5, HY zeolite, spent FCC catalyst, and the non-catalytic baseline.

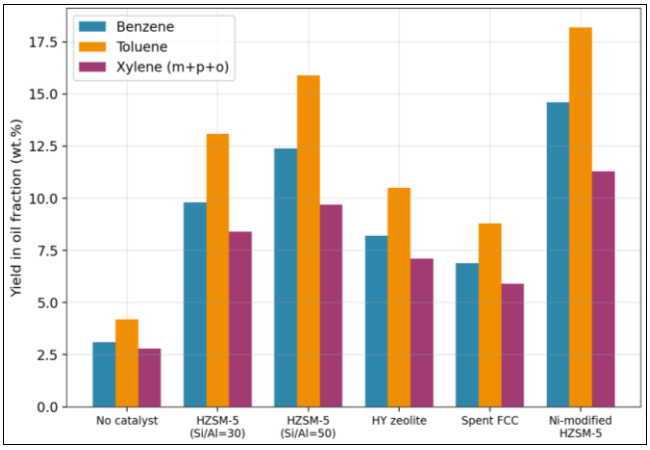

Fig 17: Effect of catalyst formulation on BTX (benzene-toluene-xylene) high-purity chemical feedstock yield

3.7 Optimization algorithm convergence behavior

Convergence diagnostics for the NSGA-II runs (Fig 18) show the hypervolume indicator rising steeply over the first 50–70 generations before plateauing near a normalized value of 0.95, while the spacing metric decreased and stabilized over a similar generation range, together indicating a well-converged, evenly distributed Pareto front for both optimization formulations.

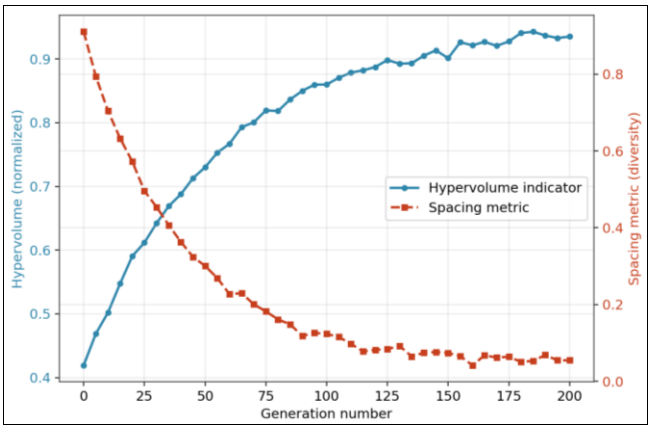

Fig 18: NSGA-II convergence behavior: hypervolume and solution-spacing metrics over 200 generations (population = 120)

4. Discussion

This study illustrates the conceptual advantage of coupling machine learning surrogate modeling with multi-objective optimization when a single thermochemical process must serve several, partly conflicting, valorization targets. Rather than optimizing pyrolysis conditions solely for maximum liquid yield, the NSGA-II framework made explicit the trade-offs between yield, lubricant viscosity index, and BTX aromatic purity, and identified compromise operating windows that a purely yield-maximizing design strategy would not surface.

The interpretability analysis is a central methodological contribution: identifying pyrolysis temperature, feedstock PE fraction, and residence time as the dominant drivers of oil yield gives process engineers a small set of variables to prioritize for real-world control and monitoring, rather than requiring simultaneous fine control of every process parameter. This mirrors the broader observation in the pyrolysis literature that a small number of variables typically dominate product distribution, even though many secondary variables (heating rate, particle size, reactor pressure) modulate outcomes at the margin.

The three downstream valorization assessments - lubricant viscosity index, bitumen-blend specification compliance, and BTX purity - indicate that a single optimized pyrolysis platform could plausibly be redirected toward different product slates depending on market conditions, simply by adjusting catalyst formulation and process severity within the explored envelope. This flexibility is attractive from a circular-economy standpoint, as it reduces the capital risk associated with committing a pyrolysis facility to a single product outlet.

A proposed primary-data version of this study would require substantial validation. Process response functions should be re-estimated from real experimental campaigns spanning the same variable ranges; downstream oil, bitumen, and BTX properties should be measured directly rather than from correlations; and the machine learning models should be retrained and re-validated on real, potentially noisier and more heterogeneous, feedstock data. Several limitations should be emphasized. The dataset assumes a relatively narrow feedstock envelope and does not capture moisture, ash, or mixed-paper contamination typical of real municipal collection streams. Third, techno-economic and life-cycle considerations were not incorporated into the optimization

objectives. Finally, extrapolation of the ML surrogate models beyond the sampled process envelope should be treated cautiously, consistent with the learning-curve behavior in Fig 10.

Despite these limitations, the workflow presented here is directly actionable: a real investigation could begin with a modest experimental design-of-experiments campaign across the variable ranges in Table 1, followed by the same ML benchmarking, SHAP interpretation, and NSGA-II optimization steps demonstrated in this example.

5. Conclusion

This study illustrates an integrated analytics workflow for waste plastic pyrolysis that couples machine learning surrogate modeling with multi-objective evolutionary optimization to jointly address three non-fuel valorization pathways: lubricant base-oil production, road-construction bitumen modification, and high-purity BTX chemical feedstock recovery. Pyrolysis temperature, feedstock PE fraction, and vapor residence time were identified as the dominant process variables governing liquid oil yield, and XGBoost provided the best predictive performance among seven benchmarked regressors (R^2 = 0.951, RMSE = 2.18 wt.%). NSGA-II multi-objective optimization successfully mapped Pareto-optimal trade-offs between oil yield and lubricant viscosity index, and between specific energy consumption and BTX aromatic purity, while downstream property simulations indicated that optimized process conditions could plausibly yield a lubricant base oil comparable to commercial Group I mineral oils, a specification-compliant modified bitumen blend, and a Ni-modified HZSM-5 catalyzed BTX yield of approximately 44 wt.% of the recovered oil fraction. Because all data underlying this paper are synthetic, these specific numerical results should be understood as illustrative of method and reporting structure rather than as validated scientific findings; the framework itself, however, defines a practical and directly transferable blueprint for a future primary-data investigation.

6. Declarations

Ethics approval: Not applicable to this manuscript, as no human participants, animal subjects experimental data were involved. Any future primary-data study built on this framework would require appropriate institutional and environmental-safety approvals.

Conflicts of interest: The authors declare no conflicts of interest.

7. References

1. Al-Salem SM, Antelava A, Constantinou A, Manos G, Dutta A. A review on thermal and catalytic pyrolysis of plastic solid waste (PSW). J Environ Manage. 2017; 197:177-198.
2. Butler E, Devlin G, McDonnell K. Waste polyolefins to liquid fuels via pyrolysis: Review of commercial state-of-the-art and recent laboratory research. Waste Biomass Valorization. 2011; 2(3):227-255.
3. Chandrasekaran SR, Kunwar B, Moser BR, Rajagopalan N, Sharma BK. Catalytic thermal cracking of postconsumer waste plastics to fuel: Kinetics and optimization. Energy Fuels. 2015; 29(9):6068-6077.
4. Chen T, Guestrin C. XGBoost: A scalable tree boosting system. Proc 22nd ACM SIGKDD Int Conf Knowl Discov Data Min, 2016, 785-794.
5. Deb K, Pratap A, Agarwal S, Meyarivan T. A fast and elitist multiobjective genetic algorithm: NSGA-II. IEEE Trans Evol Comput. 2002; 6(2):182-197.
6. Lundberg SM, Lee SI. A unified approach to interpreting model predictions. Adv Neural Inf Process Syst. 2017; 30:4765-4774.
7. Miandad R, Barakat MA, Aburiazaiza AS, Rehan M, Nizami AS. Catalytic pyrolysis of plastic waste: A review. Process Saf Environ Prot. 2016; 102:822-838.
8. Panda AK, Singh RK, Mishra DK. Thermolysis of waste plastics to liquid fuel: A suitable method for plastic waste management and manufacture of value added products. Renew Sustain Energy Rev. 2010; 14(1):233-248.
9. Singh RK, Ruj B, Sadhukhan AK, Gupta P. Impact of fast and slow pyrolysis on the degradation of mixed plastic waste: Product yield analysis and their characterization. J Energy Inst. 2019; 92(6):1647-1657.
10. Sonawane YB, Shindikar MR, Khaladkar MY. Utilization of waste plastic pyrolysis oil in bituminous road construction. Int J Sci Eng Res. 2018; 9(3):1-6.